Duplex Stainless Steels

Edited by
Iris Alvarez-Armas
Suzanne Degallaix-Moreuil

ISTE
WILEY

Duplex Stainless Steels

Duplex Stainless Steels

Edited by
Iris Alvarez-Armas
Suzanne Degallaix-Moreuil

ISTE
WILEY

First published in Great Britain and the United States in 2009 by ISTE Ltd and John Wiley & Sons, Inc.

ISTE Ltd
27-37 St George's Road
London SW19 4EU
UK

www.iste.co.uk

John Wiley & Sons, Inc.
111 River Street
Hoboken, NJ 07030
USA

www.wiley.com

Library of Congress Cataloging-in-Publication Data

Duplex stainless steels / edited by Iris Alvarez-Armas, Suzanne Degallaix-Moreuil.
p. cm.
Includes bibliographical references and index.
ISBN 978-1-84821-137-7
1. Duplex stainless steel. I. Alvarez-Armas, Iris. II. Degallaix-Moreuil, Suzanne.
TN757.C5D87 2009
672--dc22

2009026201

British Library Cataloguing-in-Publication Data
A CIP record for this book is available from the British Library
ISBN: 978-1-84821-137-7

Printed and bound in Great Britain by CPI/Antony Rowe, Chippenham and Eastbourne.

Table of Contents

Preface

Duplex stainless steels (DSSs) are chromium-nickel-molybdenum-iron bi-phased alloys in which the proportions of the constituent elements enable the optimization of the balance of the volume fractions of austenite and ferrite. Due to their ferritic-austenitic bi-phased microstructure, they possess higher mechanical strength and better corrosion resistance than standard austenitic stainless steels. Nowadays, the applications and markets for DSSs are increasing continuously, due to their outstanding properties and their relatively low cost.

The use of DSS has drastically grown in the last 10 years, particularly in the oil and gas, the pulp and paper, and chemical industries, and in chemical tankers. In all these examples, properties, such as welding, corrosion resistance, and mechanical strength, are crucial. Recent publications have also emphasized the importance of the fabrication process, as well as the effect of aging, on fracture and long-term mechanical properties, such as fatigue of DSSs; a subject that is hardly dealt with in Gunn's[1] book.

Since the edition of the book by Robert Gunn, there have been important advances in the knowledge of the DSSs, as revealed by the extensive research in the scientific literature on a wide range of topics relating to DSSs. The significance of the DSSs is reflected by the fact that the International Conference DUPLEX 2007 is the fourth conference on the subject since the publication of Gunn's book, in a series of seven since the first St Louis, USA, in 1982.

The intention of the present book is to review the most updated progress achieved in the last 10 years regarding the microstructure, corrosion resistance, and mechanical strength properties of DSSs, as well as highlighting the industrial

---

1 Gunn R.N., Ed., *Duplex Stainless Steels, Microstructure, Properties and Applications*, Abington publishing, Cambridge, 1997.

applications as a result of the development of new grades. The different subjects are developed in chapters written by world-renowned experts among the industrial and scientific communities:

Chapter 1 analyzes the impact of different microstructural variables on the hot workability of DSSs.

Chapter 2 focuses on corrosion-resistance properties and in-service properties of standard and newly developed duplex grades.

Chapter 3 describes the phase transformations that take place from the liquid state down to subzero temperatures, related microstructures, and their influence on mechanical and corrosion properties.

Chapter 4 analyzes the effect of thermal histories induced by welding processes on the austenitic-ferritic microstructure, as well as the secondary-phase precipitations. It is also proposed a guideline regarding the choice of material, process, and filler metal, in order to obtain sound welds, both in terms of corrosion resistance and mechanical properties.

Chapter 5 provides general information related to the elaboration of cast DSS and a review of the mechanisms of embrittlement occurring during aging in the temperature range 300-500°C and the consequences on fracture mechanical properties. Models of the heterogenity and size effects on the fracture result scatter are also provided.

Chapters 6 and 7 describe the cyclic plastic behavior and the dislocation structure evolution in DSSs tested under cyclic uniaxial (tension-compression) and multiaxial (tension-compression-torsion) cyclic loading at room temperature.

Chapter 8 discusses the cyclic accommodation mechanisms in a DSS from AFM measurements of the surface topography created in the two phases. It highlights the role played by each phase – austenite and ferrite – on the macroscopic behavior and provides an explanation of how they interact.

Chapter 9 discusses the modeling on different scales of monotonic and cyclic plastic behavior at room temperature observed in a hot-forged DSS.

Chapter 10 studies and compares the cyclic plastic behavior, the fatigue lifetimes, and the dislocation structures of different generations of DSSs in the as-received and aged conditions between 20 and 500°C.

Chapter 11 concisely summarizes the basics of the industrial production of DSSs and their effects on crystallographic and microstructural properties leading to differences in fatigue resistance.

Chapter 12 presents the large variety of application fields of different DSS grades and, in particular, the new DSSs.

Finally, an appendix summarizes the chemical composition of the different families of DSSs, including both cast and wrought austenitic and DSSs, and provides the designations from the different nomenclatural systems.

The Editors are grateful to all the authors who have kindly contributed to this book, especially for their effort and personal time invested in the writing of their contribution.

Iris ALVAREZ-ARMAS
Suzanne DEGALLAIX-MOREUIL

Chapter 1

Process: Hot Workability

1.1. Introduction

The advantageous performance of duplex stainless steels in many applications, when compared with other stainless steels, is directly related to their austeno-ferritic microstructure [FLO 68, SOL 83, BER 91, COM 91, NIL 92A, NIL 92B]. However, the biggest difficulties in processing duplex stainless steels arise during hot working as a direct consequence of this same austeno-ferritic microstructure [IZA 07]. In general, duplex stainless steels have poor hot workability, which consequently leads to a relatively narrow processing window. This raises difficulties during their industrial processing and the severity of the problem often produces defects seen immediately in the hot rolled material or only detected in the finished product.

The different metallurgical factors behind the hot workability of duplex stainless steels are reviewed in this paper.

1.2. As-cast microstructure

In general, duplex stainless steels of practical interest solidify to δ-ferrite, leading to the primary as-cast pattern shown schematically in Figure 1.1a in which a shell of small equiaxed grains in contact with the cast surface is followed by several

---

Chapter written by Isabel GUTIERREZ and Amaia IZA-MENDIA.

millimeter long columnar grains and finally coarse equiaxed grains at the center of the cast.

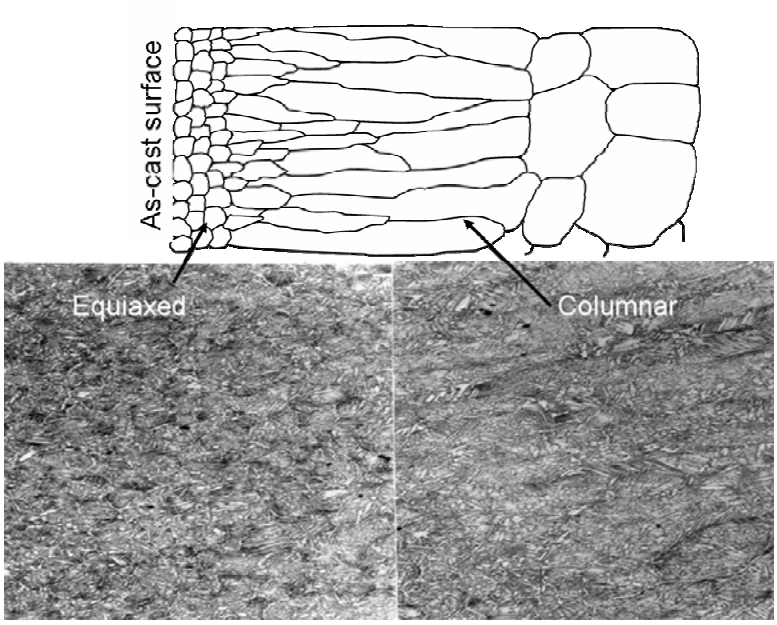

Figure 1.1. *a) Diagram showing standard as-cast grain distribution across the section and b) resultant duplex as-cast microstructure after cooling [GAR 03]*

Duplex as-cast microstructures form during the cooling as a consequence of solid state precipitation of austenite ridges at δ prior grain boundaries and Widmanstätten microstructure inside the δ-ferrite grains, as seen in Figure 1.1b. The result is a distribution of plate-like austenite monocrystals oriented in space almost at random within a polycrystalline ferrite matrix, as seen in Figure 1.2a.

Widmanstätten austenite, like its homonymous ferrite, involves a combination of some diffusive and displacive transformations [OHM 95]. This kind of solid-state transformation imposes an orientation relationship of the type Kurdjumov-Sachs (K-S) or Nishiyama-Wasserman (N-W) between the new austenite and the parent ferrite [SOL 83, IZA 97A, IZA 98], as seen in Figure 1.3, lead to semi-coherent interphase boundaries [POR 92] due to lattice plane correspondences:

$$\text{K-S: } (\mathbf{011})_{\text{Ferrite}} // (\mathbf{111})_{\text{austenite}} \text{ and } [\mathbf{11\bar{1}}]_{\text{Ferrite}} // [\mathbf{10\bar{1}}]_{\text{austenite}}$$

from which N-W can be generated by a rotation of 5.26° about $[011]_{\text{Ferrite}}$.

The austenite ridges at ferrite grain boundaries maintain this same type of orientation relationship with one of the ferrite grains while the other interphase boundary is incoherent.

The isothermal kinetics of the austenite precipitation can be expressed by an Avrami-type equation [SOU 80]. However, under non-isothermal conditions, the cooling rate has a great effect on the morphology and amount of precipitated austenite. Widmanstätten-type growth takes place below 1,000°C [OHM 95] and it has been reported that it can be suppressed in a deformed microstructure when cooling at a rate higher than 2°C/s. However, in the absence of deformation high cooling rates enhance such types of transformation [KAU 93].

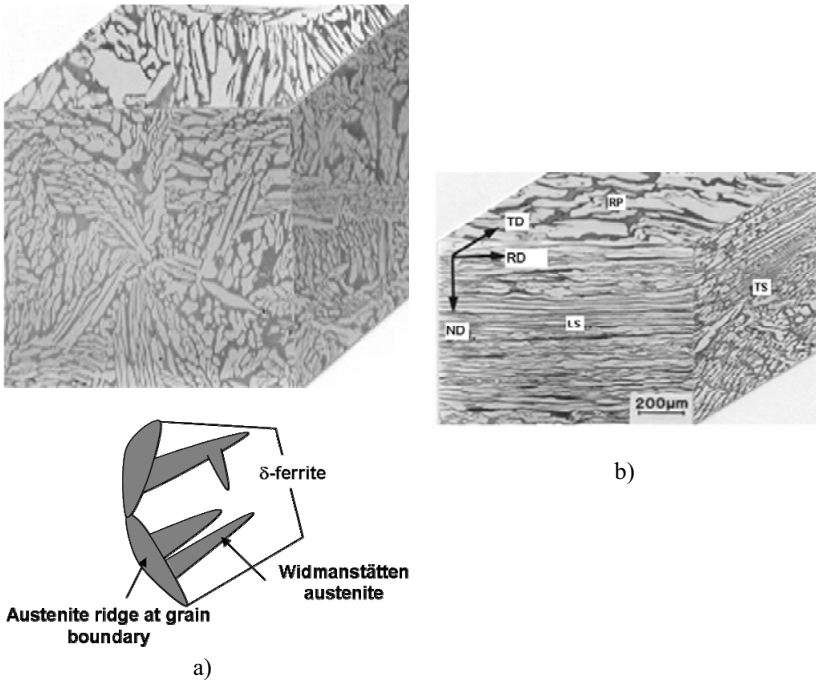

Figure 1.2. *3D reconstruction made from optical images of the a) equiaxed region of as-cast microstructure and diagram showing the austenite morphology and b) wrought microstructure after 77% hot reduction of the same duplex stainless steel. The rolling plane (RP), longitudinal section (LS) and transverse section (TS) [PIÑ 97] are also indicated*

Atamert and King [ATA 92] devised an equation for welding by relating the volume fraction of austenite to the difference between Cr_{eq} and Ni_{eq} and the cooling time between 1,250 and 800°C. Similar approaches or continuous cooling-phase

transformation models allow us to predict the fraction of austenite after continuous/ingot casting [GOB 07]. However, it should be noted that, when the as-cast material is cooled and subsequently reheated at a high temperature before hot working, the relevant microstructure is the actual structure present at this stage and evolving throughout the whole process.

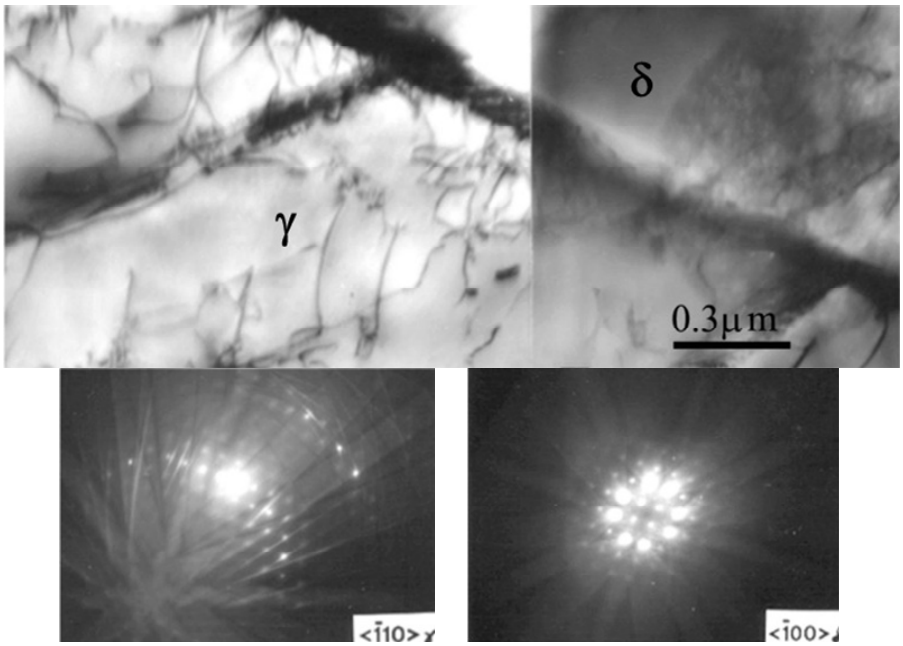

Figure 1.3. *K-S orientation relationship between austenite and parent δ-ferrite in the as-cast microstructure [IZA 99]*

1.3. Microstructural evolution during hot working

The process of industrial hot rolling begins with a reheating stage at around 1,250°C [BOT 96, DUP 02A]. This stage acts as a solution treatment leading to a certain phase balance depending on the steel composition, as seen in Figure 1.4. However, given that an important fraction of austenite remains undissolved at reheating temperatures for commercial compositions, the as-cast microstructure is preserved to some extent. Increasing the holding time has been reported to induce a degree of globulization of the austenite phase [GOB 07].

Hot rolling transforms this microstructure to a planar linear configuration, as illustrated in Figure 1.2b. After a 70% hot rolling reduction, the microstructure has a

fibrous appearance throughout the longitudinal section: long austenite stringers distributed in a ferritic matrix. In other sections, the austenite appears more dispersedly distributed. The size of the austenite stringers and the separation between them vary from region to region. Additionally, at certain locations, some units lose the general alignment and/or present a blocky aspect. Lower rolling reductions produce microstructures that are midway between as-cast and the wrought one shown in Figure 1.2b.

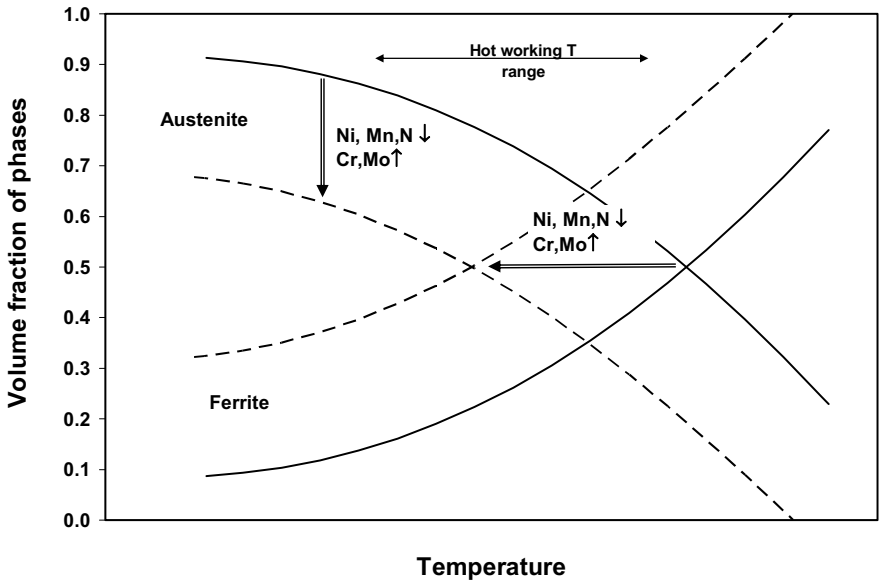

Figure 1.4. *Diagram showing the effect of temperature and steel composition on the phase balance*

Although the development of an oriented microstructure is the most evident microstructural change produced by hot rolling, a detailed analysis of the evolution of a duplex microstructure requires at least three different levels:

– distribution, shape, volume fraction, and phase size;

– interphase boundaries and eventual orientation relationships;

– grain microstructure within each phase and associated textures and/or mesotextures.

1.3.1. *Changes in morphology and distribution of the dispersed γ phase*

The use of marked specimens to perform thermomechanical simulations in the laboratory, followed by microstructural observations [PIÑ 99, PIÑ 00A] enabled the identification of several mechanisms that modify the shape and distribution of the austenite. Some of the mechanisms listed in Figure 1.5 account for plastic deformation, whereas others are the result of strain partitioning, strain localization, some phase accommodation, and microstructural changes towards equilibrium.

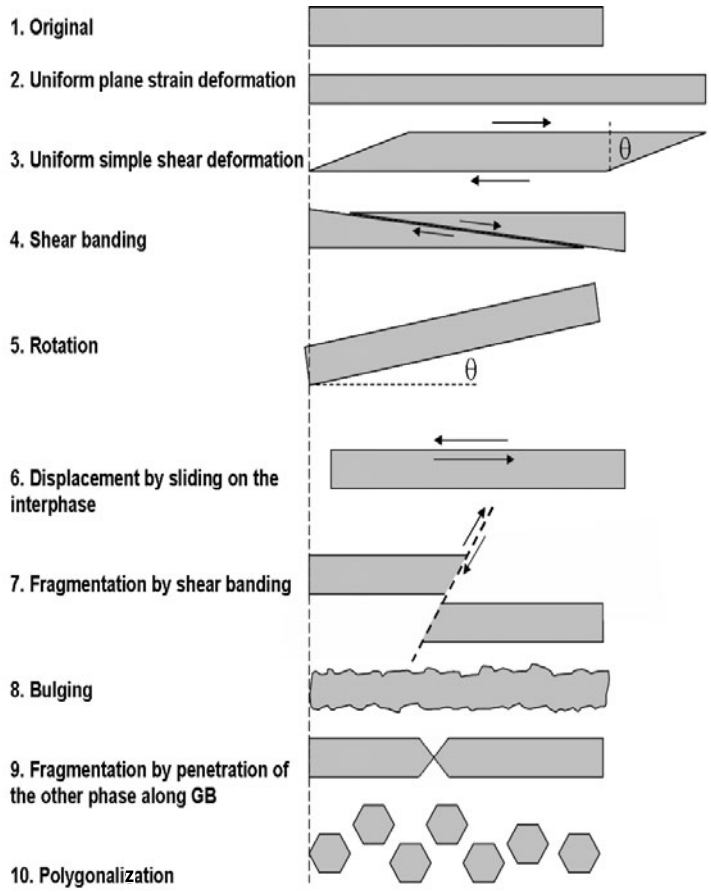

Figure 1.5. *Mechanisms acting on the disperse phase that are responsible for the morphological and distribution changes undergone by the austenite during hot working of austeno-ferritic stainless steels (grain boundary)*

1.3.2. *Plastic deformation*

Plane strain and pure shear are the only mechanisms that account for the uniform plastic deformation of both ferrite and austenite. The microstructural evolution taking place during hot working within both phases in a duplex microstructure can significantly differ from that observed in single-phase materials. This is because, in addition to their respective high (ferrite) and low (austenite) stacking fault energies, other factors, such as relative strength, morphology, and strain partitioning, also play an important role.

Ferrite: Ferritic stainless steels undergo dynamic recovery [SEL 76, MCQ 96, URC 87, EVA 91, LOM 81] and develop a well-defined subgrain microstructure quite early that remains equiaxed and of constant size once a steady state is reached. In an austeno-ferritic microstructure, dynamic recovery is the primary softening mechanism activated in ferrite [IZA 97B, CIZ 06, DEH 07], see subgrains in Figure 1.6. The ferrite substructure becomes more polygonalized at higher deformations and low strain rates. However, the interphase boundary imposes some restrictions and, as the strain increases, ferrite becomes partially entrapped between γ stringers. The thickness of ferrite (distance between γ stringers) decreases with increasing strain, until it becomes comparable with the ferrite subgrain size.

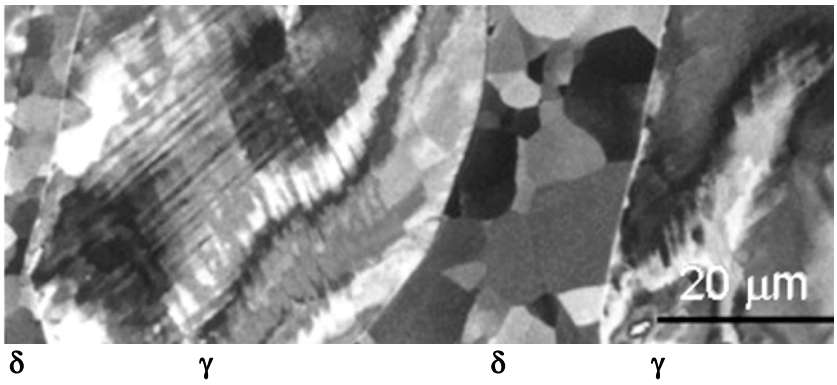

Figure 1.6. *Scanning electron microscopy backscattered electron image of as-cast 2304 duplex stainless steel deformed at 1,000°C and 1s^{-1} to a strain ε=1 [IZA 99]*

This is a quite heterogenous process that leads to a bamboo-type structure, as illustrated in Figure 1.7, forming narrow bands of ferrite, limited laterally by the interphase boundaries and subdivided by a mixture of low and high-angle ferrite-ferrite boundaries. The mechanism responsible for the formation of high-angle homophase boundaries in ferrite has been attributed to continuous dynamic

recrystallization [IZA 97B, DEH 07], geometric dynamic recrystallization [EVA 04], or extended dynamic recovery [CIZ 06].

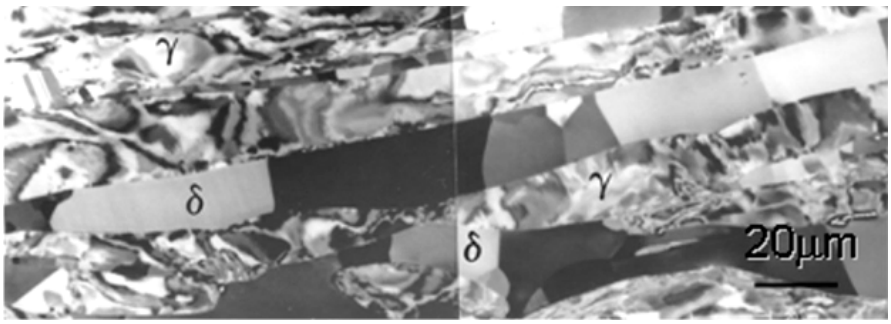

Figure 1.7. *Scanning electron microscopy backscattered electron image showing δ with bamboo-type structure. As-cast 2205 steel deformed by plane strain compression (PSC) at 1,000°C and 1s^{-1} to ε=1.2 [IZA 99]*

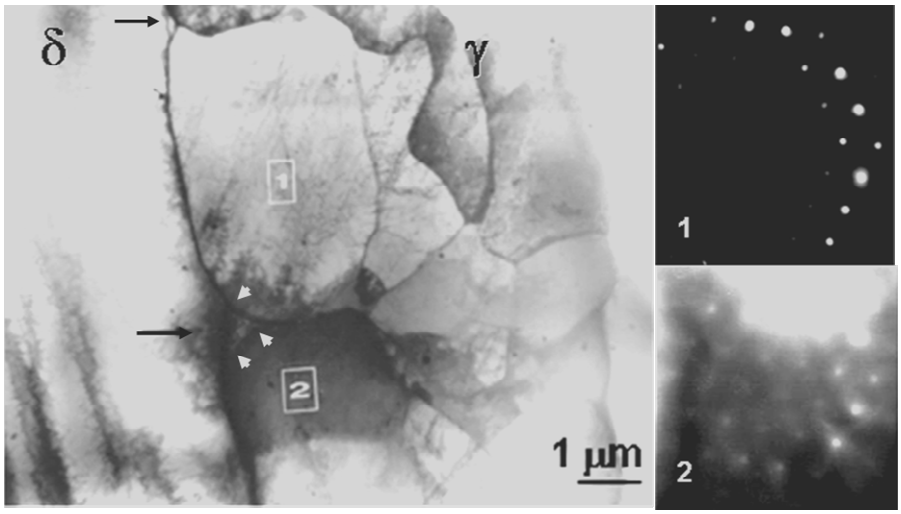

Figure 1.8. *Transmission electron microscopy image and diffraction patterns corresponding to two subgrains in austenite. Steel 2205 deformed at 1,200°C and 1s^{-1} to ε=1.76 [IZA 99]*

Austenite: Due to their low stacking fault energy, austenitic steels undergo significant work hardening before the onset of dynamic recrystallization at hot working temperatures [MCQ 75, BAR 79, AHL 82, RYA 90, VEN 94, JOR 05]. The flow curves of the duplex stainless steel frequently exhibit a strain-hardening stage, and then reach a peak followed by some softening [IZA 97A]. Such behavior

has sometimes been attributed to the occurrence of dynamic recrystallization of the austenite. However, microstructural observations prove otherwise. Misorientation analysis shows that, even at high deformation temperatures, dynamic recrystallization does not occur even at strains well beyond the peak [IZA 97A, IZA 98]. Furthermore, when it is observed it reaches negligible volume fractions [DEH 07]. The level of the dynamic recovery in γ-phase increases with rising temperature and decreasing strain rate. In fact, when deforming an austeno-ferritic microstructure at temperatures around 1,000°C, the austenite remains structureless at low strains and progressively develops a tangled microstructure as the strain increases, as illustrated in Figure 1.6.

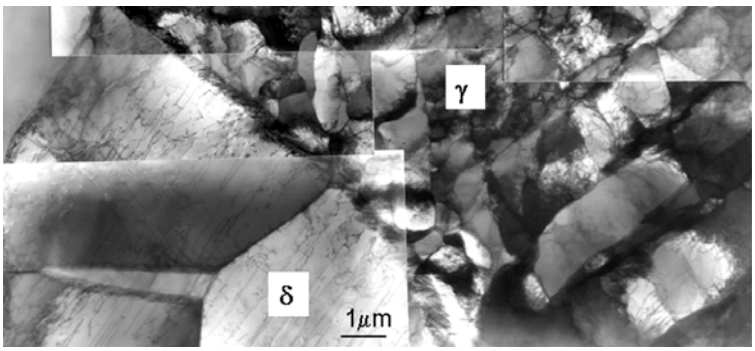

Figure 1.9. *Transmission electron microscopy image showing different degrees of recovery in ferrite and in austenite. Wrought 2304 steel with a globular structure deformed at 1,000°C $1s^{-1}$ to a strain ε=1.4 [IZA 99]*

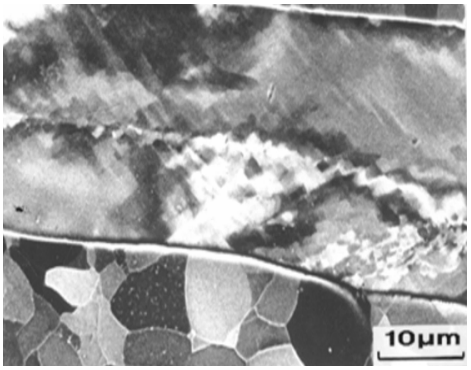

Figure 1.10. *Scanning electron microscopy backscattered electron image showing a micro shear band in austenite. As-cast 2304 steel deformed at 1,000°C and $1s^{-1}$ to a strain ε=1.6 [IZA 99]*

At 1,100°C and above, cells and subgrains form within the austenite. An example of well-developed subgrain within an austenite stringer is shown in the transmission electron microscopy (TEM) image in Figure 1.8. Independently of deformation conditions, the degree of recovery during hot working is always higher in δ than in γ: austenite always exhibits cells/subgrains smaller in size than ferrite subgrains, as depicted in Figure 1.9. The strain distributes quite heterogenously from place to place. A degree of microshear banding is often observed within austenite units at the transition between regions in which different slip systems have activated, as seen in Figure 1.10.

Interphase boundary coherency: The development of high-angle boundaries in ferrite involves some lattice rotations that significantly change the character of the ferrite-austenite interphase boundaries, as illustrated in Figure 1.11 [IZA 99]. The channeling contrast image shows a ferrite unit located between two austenite grains. The central part of ferrite in the image has a zone axis close to $<359>_{\delta}$ and maintains the K-S orientation within a deviation of 3-6° with austenite at each side. The upper part of the ferrite in the image has developed subgrains with a zone axis close to $<111>_{\delta}$. The lattice rotation between the two ferrite zone axes can be described approximately by 24° around a $<122>_{\delta}$ axis. As a result of such rotation the initial K-S orientation relationship present in the as-cast microstructure between ferrite and austenite is lost locally and random interphase boundary segments have developed.

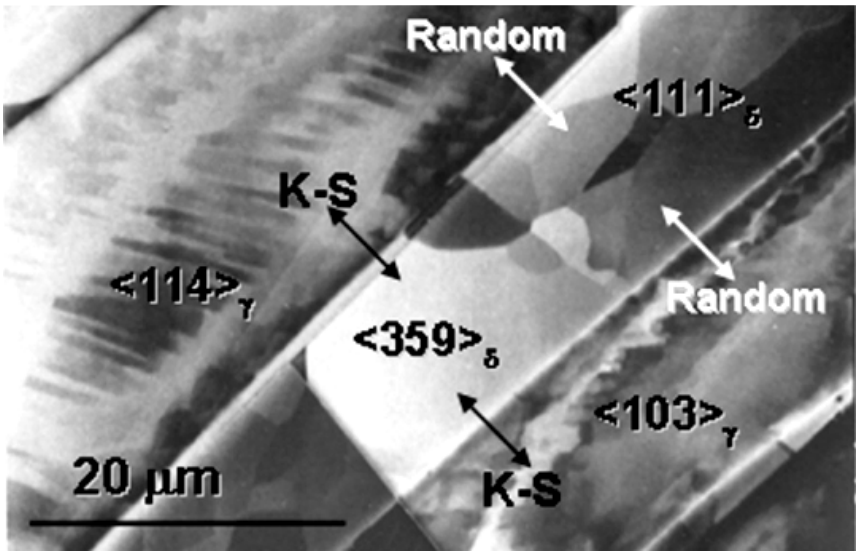

Figure 1.11. *STEM channeling image and crystallographic orientation analysis. As-cast 2304 steel deformed at 1,000°C and $1s^{-1}$ to a strain ε=1.6 [IZA 99]*

Interphase boundary mobility: When deforming at 1,000°C or even at lower temperatures, the interphase boundary remains perfectly flat, as illustrated in Figure 1.11. However, as the deformation temperature increases, the interphases become mobile and bulges develop. The perturbations of the interphase take place on a small scale (fractions of micron) and lead to some interpenetration of both ferrite in austenite or austenite in ferrite. The TEM image in Figure 1.8 illustrates how two γ subgrains bulge (point 8 in Figure 1.5) from austenite and produce a sharp triple point formed by the common subgrain boundary and the interphase (see arrows). This example is a clear exponent of the fact that bulging is not related to dynamic recrystallization in an austeno-ferritic microstructure in contrast to what happens in austenitic steels. Sharp triple points also form at the intersection between the interphase boundary and ferrite-ferrite single-phase grain boundaries, which are almost perpendicular to it, as shown in Figure 1.12 (point 9 in Figure 1.5).

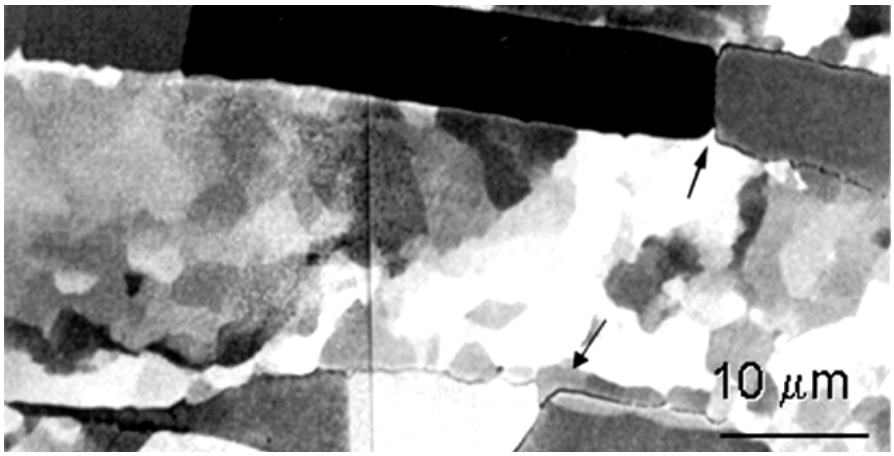

Figure 1.12. *Scanning electron microscopy backscattered electron image showing irregularities at austenite-ferrite interphases. As-cast 2304 steel deformed at 1,200°C and 1s^{-1} to a strain ε=1.6 [IZA 99]*

1.3.3. *Rotation*

Apart from the lattice rotations taking place on a substructural scale, such as those illustrated in Figure 1.12, marked specimens reveal macroscopic phase rotations (point 5 in Figure 1.5). The marks in Figure 1.13 clearly illustrate that the austenite in the middle of the image has rotated as a whole within the ferrite matrix, which has simultaneously experienced intense local shearing [PIÑ 03].

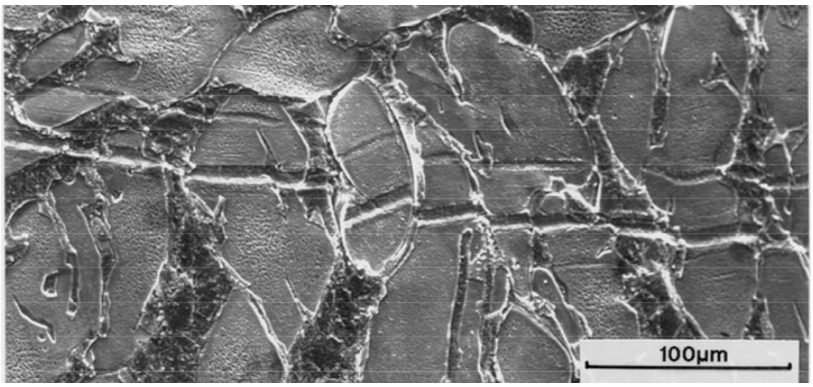

Figure 1.13. *SEM image showing the rotation of an austenite unit outlined by the displacement of the scratch markers at the specimen surface. As-cast material deformed by torsion at 1,000°C and 1s^{-1} to a strain of 1.6 [PIÑ 03]*

1.3.4. *Interphase boundary sliding*

Sliding involves the translation of a grain with respect to another by a shear movement parallel to their common boundary [ALD 67, MUR 75] (point 6 in Figure 1.5). Sliding has been identified in hot-worked, as-cast and wrought duplex stainless specimens, aided by metallographic characterization after deformation of pre-polished and marked specimens [PIÑ 00A].

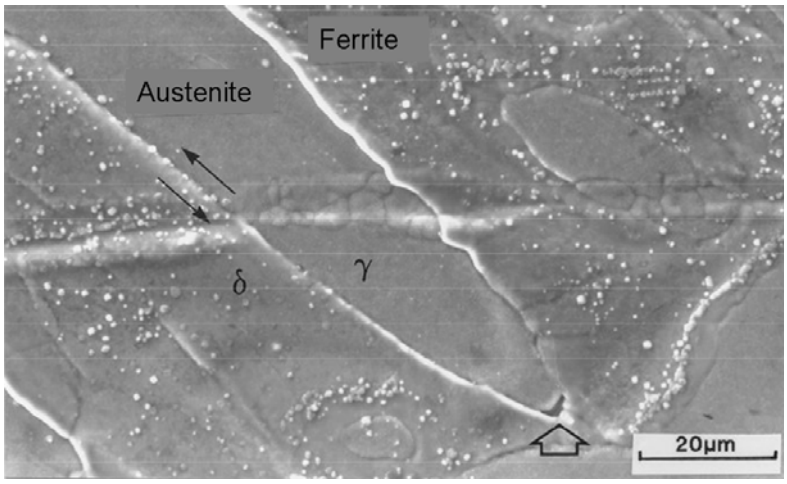

Figure 1.14. *A clear example of interphase boundary sliding leading to some damage formation [PIÑ 99]*